ELSEVIER

Journal of Magnetism and Magnetic Materials 232 (2001) 139–146

Journal of magnetism and magnetic materials

www.elsevier.com/locate/jmmm

Magnetic structure of the ternary germanide $Ce_3Ni_2Ge_7$

L. Durivault[a,b], F. Bourée[a], B. Chevalier[b,*], G. André[a], J. Etourneau[b], O. Isnard[c]

[a] *Laboratoire Léon Brillouin (CEA-CNRS), CEA/Saclay, 91191 Gif-sur-Yvette, France*

[b] *Institut de Chimie de la Matière Condensée de Bordeaux (ICMCB), CNRS [UPR 9048], Universite Bordeaux I, 87 Avenue du Dr. A. Schweitzer, 33608 Pessac Cedex, France*

[c] *Laboratoire de Cristallographie, CNRS, BP 166X, 38042 Grenoble, France*

Received 11 January 2001; received in revised form 15 February 2001

Abstract

The ternary germanide $Ce_3Ni_2Ge_7$ has been studied by means of neutron powder diffraction and Ce L_{III} X-ray absorption (XAS). This compound which orders antiferromagnetically below $T_N = 7.2(2)$ K, crystallizes in the orthorhombic (Cmmm space group) $La_3Co_2Sn_7$-type structure where Ce atoms occupying two inequivalent crystallographic sites: Ce1 at 2d site and Ce2 at 4i site. Below T_N, the antiferromagnetic structure of $Ce_3Ni_2Ge_7$ is collinear but only the Ce2 atoms carry a magnetic moment ($1.98(2)\,\mu_B$ at 1.4 K). The absence of ordered magnetic moment on Ce1 atoms can be correlated to the average valence $v = 3.03(1)$, determined by X-ray absorption spectroscopy, suggesting an intermediate valence state of cerium in the 2d site.

PACS: 6112; 7550.E

Keywords: Ternary germanide; Antiferromagnet; Intermediate valence; Magnetic structure

1. Introduction

The ternary compounds $Ce_3Ni_2Ge_7$ and $Ce_3Ni_2Sn_7$ crystallize in the orthorhombic $La_3Co_2Sn_7$-type structure (Cmmm space group) where Ce atoms occupy two different sites [1,2]. Recent investigation of these intermetallics by electrical resistivity and magnetization measurements shows that $Ce_3Ni_2Ge_7$ orders antiferromagnetically below $T_N = 7.0(2)$ K, a Néel temperature higher than that observed for $Ce_3Ni_2Sn_7$ ($T_N = 3.8(2)$ K) [3]. This result appears surprising because as a general rule, cerium–nickel based germanides are less magnetic than the homologue stannides. For instance, in the sequence CeNiGe→CeNiSn (orthorhombic TiNiSi-type), a transition from an intermediate valence state to Kondo semiconductor behaviour is observed [4,5]; in the same way $CeNi_2Ge_2$ is considered as a non-ordered 'heavy-fermion' compound showing the occurrence of superconductivity under pressure [6] whereas $CeNi_2Sn_2$ orders antiferromagnetically below $T_N = 1.8$ K [7,8]. All these results indicate that the J_{cf} interaction constant between the 4f(Ce) and conduction electrons which governs the competition between the demagnetizing Kondo and the magnetic RKKY interactions, is greater in

*Corresponding author. Tel.: +33-5-56-84-63-36; fax: +33-5-56-84-27-61.

E-mail address: chevalie@icmcb.u-bordeaux.fr (B. Chevalier).

0304-8853/01/$ - see front matter
PII: S0304-8853(01)00189-5

$CeNi_2Ge_2$ than in $CeNi_2Sn_2$. In this view, it is of interest to compare the valence state and the magnetic arrangement of the cerium atoms in $Ce_3Ni_2Ge_7$ and $Ce_3Ni_2Sn_7$.

In this paper, are reported the results obtained by neutron powder diffraction experiments on $Ce_3Ni_2Ge_7$ in order to determine its both crystal and magnetic structures. In addition, we have performed at room temperature Ce L_{III} edge X-ray absorption spectroscopy measurements on $Ce_3Ni_2Ge_7$ and $Ce_3Ni_2Sn_7$ in order to study the evolution of the Ce-4f electronic state in the sequence $Ce_3Ni_2Ge_7 \rightarrow Ce_3Ni_2Sn_7$.

2. Experimental procedures

$Ce_3Ni_2Ge_7$ sample was prepared by melting stoichiometric amounts of the constituents (purity > 99.9%) in an induction levitation furnace under a purified argon atmosphere. The sample was then annealed under vacuum at 800°C for 6 weeks. Its homogeneity and chemical composition were checked by microprobe analysis based on the measurements of the Ce $L_{\alpha 1}$, Ni $K_{\alpha 1}$ and Ge $K_{\alpha 1}$ X-ray emission lines, which were compared to those obtained for CeNiGe used as a reference. This analysis shows that the sample is practically a single phase; Ce_2NiGe_6 (<3–4% in mass) is detected as impurity phase.

Magnetization measurements were carried out using a superconducting quantum interference device (SQUID) magnetometer.

Neutron powder diffraction experiments were performed at the Orphée reactor (CEA/Saclay, France), on the two-axis diffractometers 3T2 (high-resolution powder diffraction; $\lambda = 0.1225$ nm) and G4-1 (800 cell-position-sensitive-detector; $\lambda = 0.2426$ nm). The data were analysed with the Rietveld profile method using the Fullprof program [9], with neutron scattering lengths and Ce^{3+} form factor respectively from Refs. [10] and [11].

The X-ray absorption experiments were performed at room temperature, in transmission mode, using the beam lines of the DCI synchrotron source at LURE (Orsay, France) working at 1.85 GeV on the EXAFS 13 experimental station. The X-rays were monochromated using two parallel Si crystals cut along the (3 1 1) plane. To remove harmonics in the Ce L_{III} edge absorption region (5690–5760 eV), the parallelism between the two Si crystals was adjusted. The energy scale was calibrated by reference to the Cr K edge absorption in chromium metal foil. For the X-ray absorption data acquisition, the samples $Ce_3Ni_2Ge_7$ and $Ce_3Ni_2Sn_7$ were ground (grain size ≈ 40 μm). Then a calibrated amount of powder sample was mixed with cellulose in order to optimize the edge jump.

3. Results and discussion

3.1. Magnetic properties

The thermal dependence of the magnetization of $Ce_3Ni_2Ge_7$, given in Fig. 1, shows a peak, typical of an antiferromagnetic ordering with $T_N = 7.2(2)$ K. This Néel temperature is close to that determined ($T_N = 7.0(2)$ K) previously for this ternary germanide [3].

We note also that the effective moment $\mu_{eff} = 2.32\,\mu_B$/Ce determined above 70 K from the Curie–Weiss law in Ref. [3] is smaller than that calculated for a free Ce^{3+} ion ($\mu_{eff} = g_J[J \times (J+1)]^{1/2} = 2.54\,\mu_B$ where $g_J = \frac{6}{7}$ is the Landé factor and $J = \frac{5}{2}$ the total angular momentum). This result, confirmed by the present study $\mu_{eff} = 2.29\,\mu_B$/Ce, suggests that at least one of the two different Ce atoms in $Ce_3Ni_2Ge_7$ is not purely trivalent.

3.2. Crystal structure

The neutron diffraction pattern of the $Ce_3Ni_2Ge_7$ sample collected at 300 K using 3T2 diffractometer is shown in Fig. 2. These diffraction data were analysed using the Rietveld technique with Fullprof program [9]. The results are summarized as follows: (i) the sample contains ≈3% (weight percentage) of the impurity phase Ce_2NiGe_6 (Amm2 space group) crystallizing in the orthorhombic Ce_2CuGe_6-type structure (the lattice parameters of this ternary germanide were taken from Ref. [1]); (ii) $Ce_3Ni_2Ge_7$ adopts the orthorhombic $La_3Co_2Sn_7$-type structure with

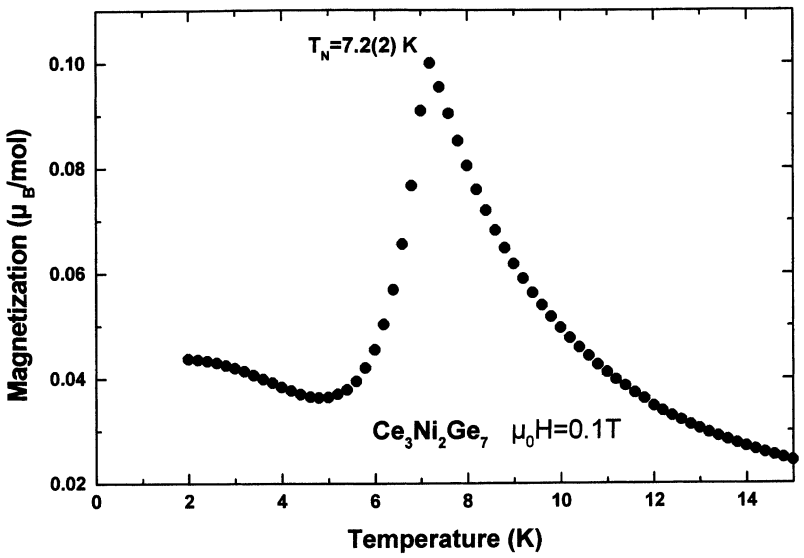

Fig. 1. Thermal dependence of the magnetization of $Ce_3Ni_2Ge_7$ measured in an applied field of $\mu_0 H = 0.1\,\mathrm{T}$.

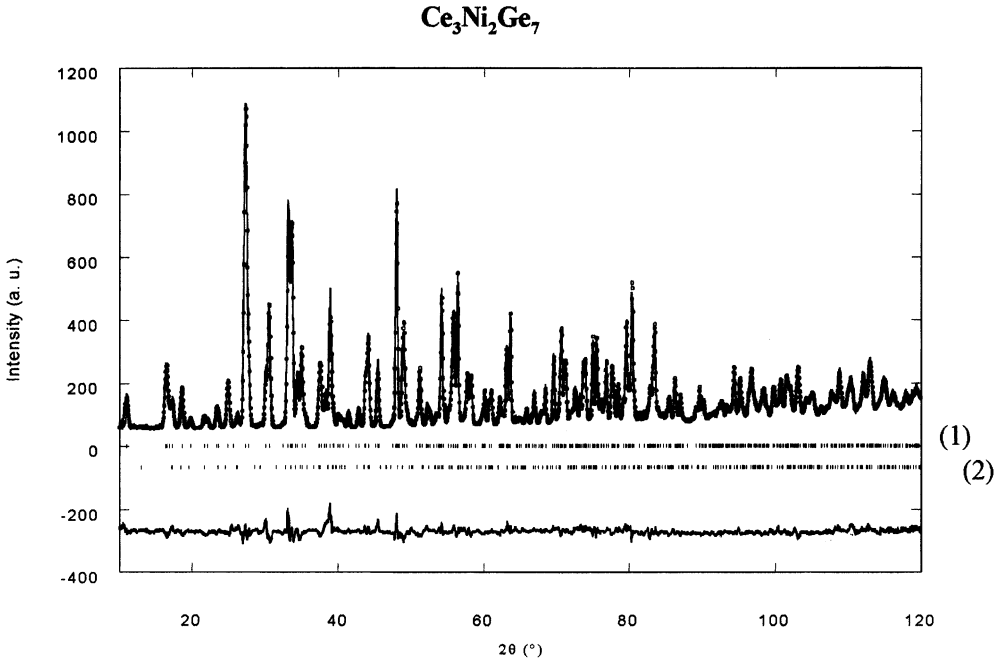

Fig. 2. Neutron powder diffraction pattern ($\lambda = 0.1225\,\mathrm{nm}$) of $Ce_3Ni_2Ge_7$ at 300 K. The dots represent the observed data points; the solid lines reveal the calculated profile and the difference (bottom) between observed and calculated profiles. The ticks correspond to 2θ Bragg positions for $Ce_3Ni_2Ge_7$ (1) and Ce_2NiGe_6 (2).

$a = 0.42327(6)$ nm, $b = 2.55517(4)$ nm and $c = 0.42896(5)$ nm as unit cell parameters. The refined structural and thermal parameters and the values of the reliability factors are listed in Table 1. The structural parameters are close to those determined previously for the homologue ternary stannide $Ce_3Ni_2Sn_7$ [3].

Table 1
Refined structural and isotropic thermal parameters at 300 K for $Ce_3Ni_2Ge_7$. The parameters are $a = 0.42327(6)$ nm, $b = 2.55517(4)$ nm and $c = 0.42896(5)$ nm. The reliability factors are $R_{wp} = 10.8\%$, $R_p = 10.1\%$, $R_e = 4.04\%$ and $R_B = 6.42\%$, respectively

Atom	Site	x	y	z	B_{iso} (Å^2)
Ce1	2d	0	0	1/2	0.55(8)
Ce2	4i	0	0.3169(2)	0	0.67(5)
Ni	4j	0	0.12853(6)	1/2	0.67(2)
Ge1	2b	1/2	0	0	2.46(7)
Ge2	4i	0	0.0882(1)	0	0.64(3)
Ge3	4j	0	0.4128(1)	1/2	0.74(3)
Ge4	4j	0	0.2217(1)	1/2	0.58(3)

The crystal structure of $Ce_3Ni_2Ge_7$, presented in Fig. 3a, can be seen along **b**-axis as a stacking alternated of three different polyhedra: (1) cuboctahedron [Ge_{12}] surrounding Ce1 atom, (2) antiprism [$Ce2_4Ge_4$] occupied by Ni atom and (3) trigonal prism [$Ce2_6$] within which an Ge atom is located. It is interesting to note that similar antiprism and trigonal prism constitute the crystal structure of the ternary germanide $CeNiGe_2$ which exhibits only one crystallographic site exists for Ce atoms [12,13].

In $Ce_3Ni_2Ge_7$, the two crystallographically inequivalent Ce atomic sites have different environments. It is interesting to compare the interatomic distances existing between Ce1 and Ce2 atoms with their nearest neighbours (Table 2): all

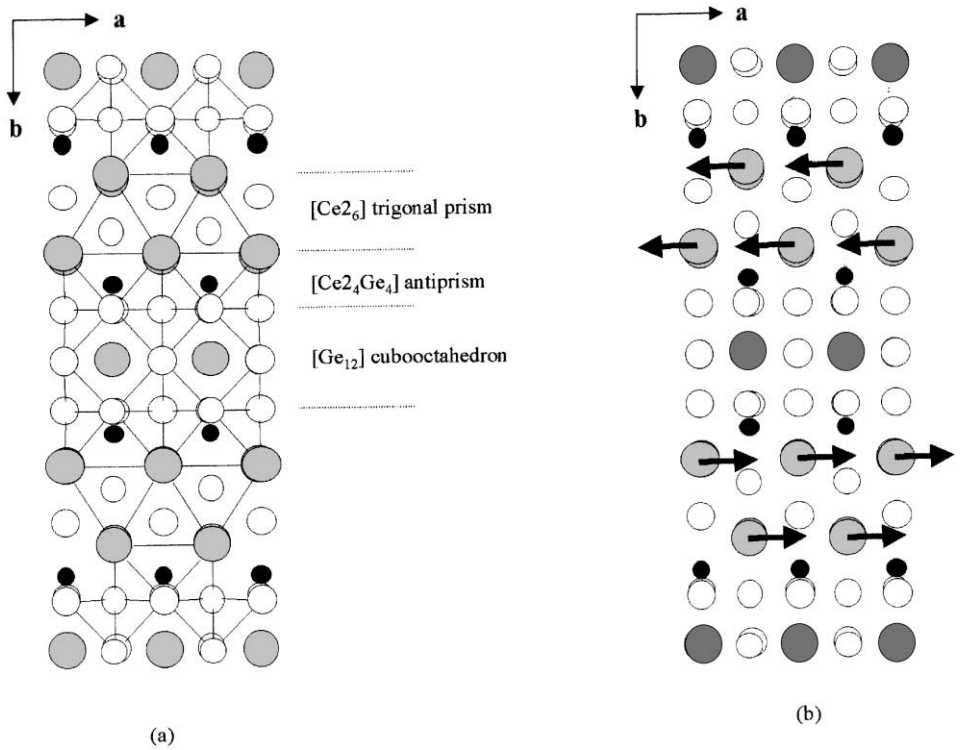

Fig. 3. (a) Projection along the **c**-axis of the crystal structure of $Ce_3Ni_2Ge_7$ (Ce, Ge and Ni are respectively represented by large grey, medium white and small black circles); (b) Projection of the magnetic structure of $Ce_3Ni_2Ge_7$ (Ce1 and Ce2 atoms are respectively represented by large dark grey and large medium grey circles).

the Ce1–Ni and Ce1–Ge distances are shorter than their homologues concerning the Ce2 atom. In other words, the mixing of 4f(Ce) orbitals with those of the Ni and Ge ligands may be favoured for Ce1 atoms. The Ce1–Ge distances are clearly smaller than those existing in $CeNi_2Ge_2$ (0.318 ($\times 8$) nm) and comparable to those determined in CeNiGe (0.298 ($\times 2$); 0.306; 0.307 and 0.321 ($\times 2$) nm) [1]. We recall that these ternary germanides $CeNi_2Ge_2$ and CeNiGe exhibit no magnetic ordering and are classified respectively as 'heavy fermion' and intermediate valence compounds [4,6]. In this view, the magnetic behaviour of the two non-equivalent Ce atoms in $Ce_3Ni_2Ge_7$ could be clearly different.

Table 2
Selected interatomic distances (nm) at $T = 300$ K in $Ce_3Ni_2Ge_7$

Ce1–Ce1	0.42327(6) ($\times 2$)	Ce2–Ce2	0.42327(6) ($\times 2$)
Ce1–Ce1	0.42896(5) ($\times 2$)	Ce2–Ce2	0.42896(5) ($\times 2$)
Ce1–Ni	0.3284(2) ($\times 2$)	Ce2–Ce2	0.4021(3) ($\times 2$)
Ce1–Ge1	0.3013 (2) ($\times 4$)	Ce2–Ni	0.3320 (2) ($\times 4$)
Ce1–Ge2	0.3111(2) ($\times 4$)	Ce2–Ge2	0.3218(3) ($\times 2$)
Ce1–Ge3	0.3073(2) ($\times 4$)	Ce2–Ge3	0.3256(3) ($\times 2$)
		Ce2–Ge4	0.3243(3) ($\times 2$)
		Ce2–Ge4	0.3170(2) ($\times 4$)

3.3. Magnetic structure

Medium resolution neutron powder diffraction patterns ($\lambda = 0.2426$ nm) for $Ce_3Ni_2Ge_7$ have been recorded in the 1.4–14.5 K low temperature range (Fig. 4). At 14.5 K, the pattern reveals reflections associated to nuclear scattering only: the unit cell parameters are then equal to $a = 0.42199(8)$ nm; $b = 2.5467(7)$ nm and $c = 0.42763(8)$ nm. At low temperature, additional Bragg peaks appear, which can be indexed in the nuclear unit cell ($a \times b \times c$) but obeying the selection rule $h + k = 2n + 1$ forbidden by the Cmmm space group relative to the crystal structure of $Ce_3Ni_2Ge_7$. Thus, the Ce ordering may be described as anti-C; i.e. Ce moments related by the C-translation $[\frac{1}{2}\frac{1}{2}0]$ are antiparallel. The magnetic structure is characterized by wave vector $\mathbf{k} = (0\,1\,0)$.

A new magnetic Bragg peak appearing at $2\theta = 6.41^\circ$ (Fig. 4), can be attributed to the presence of Ce_2NiGe_6 impurity phase in the sample. This last ternary germanide orders antiferromagnetically below $T_N = 10.4$ K [14].

Applying Bertaut's representation analysis of magnetic structures [15] to Cmmm space group, $\mathbf{k} = (0\,1\,0)$ propagation vector, leads to the existence of eight one-dimensional irreducible

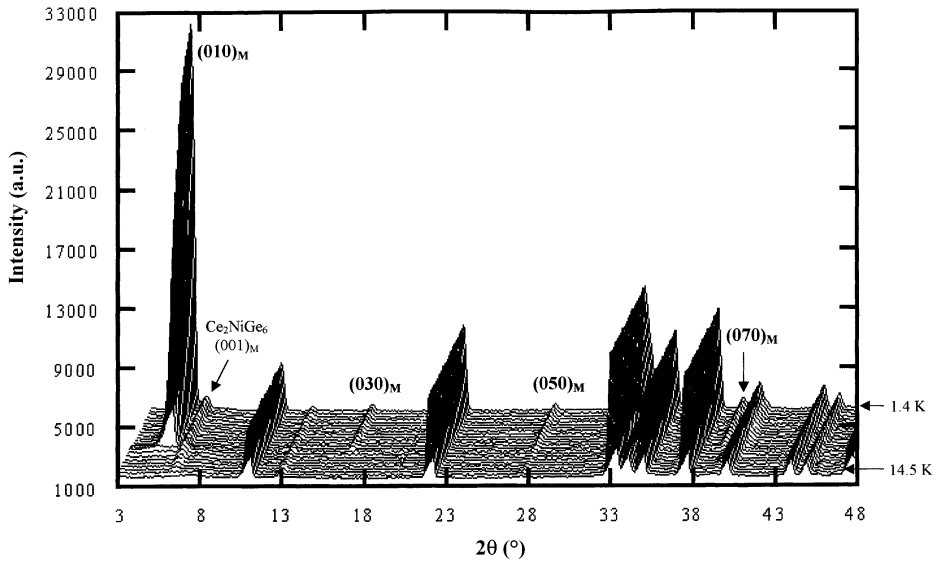

Fig. 4. Neutron powder diffraction pattern ($\lambda = 0.2426$ nm) of $Ce_3Ni_2Ge_7$ from 14.5 to 1.4 K (the magnetic peak are labelled $(h\,k\,l)_M$).

representations, hereafter called $\Gamma_1, \Gamma_2, \ldots, \Gamma_8$. The ΓCe1 and ΓCe2 matrices for transformation of Ce1 and Ce2 magnetic moments components under Cmmm symmetry elements are then reduced to:

$$\Gamma\text{Ce1} = \Gamma_3 + \Gamma_5 + \Gamma_7$$

and

$$\Gamma\text{Ce2} = \Gamma_2 + \Gamma_3 + \Gamma_4 + \Gamma_5 + \Gamma_7 + \Gamma_8.$$

The corresponding basis vectors are listed in Table 3. Only half of the magnetic atoms are included in this table, the translation [1/2 1/2 0] leading to a change in the sign of magnetic moment.

The best fit ($R_M = 4.2\%$) between observed and calculated magnetic intensities at 1.4 K (Table 4) indicates that the antiferromagnetic ordering is associated to Γ_8 irreductible representation. The magnetic moments are parallel to the **a**-axis, only the Ce2 magnetic moments are ordered, with $M_{Ce2} = 1.98(2)\,\mu_B$, close to the expected value for Ce^{3+} free ion ($g_J J = 2.14\,\mu_B$). No ordered magnetic moment is obtained on the Ce1 site.

Table 3
Bertaut's representation analysis of magnetic structures (Cmmm space group, $\boldsymbol{k} = (0\,1\,0)$ propagation vector): basis vectors for Ce1 in (2d) and Ce2 in (4i) sites ($m \neq M$)

	Ce1 [0 0 $\frac{1}{2}$)	Ce2 [0 y 0]	Ce2 [0 1 − y 0]
Γ_3	m_x	M_x	M_x
Γ_8		M_x	$-M_x$
Γ_5	m_y	M_y	M_y
Γ_2		M_y	$-M_y$
Γ_7	m_z	M_z	M_z
Γ_4		M_z	$-M_z$

Table 4
Calculated and observed magnetic intensities of $Ce_3Ni_2Ge_7$ at 1.4 K

$(h\,k\,l)_M$	$2\theta_{obs}$ (°)	$Int_{calc.}$ (a.u.)	Int_{obs} (a.u.)
010	5.46	14 597(2)	14 235
030	16.43	212(5)	152
050	27.55	149(5)	157
011	33.43	763(l)	807
120	35.26	43(2)	49
031	37.04	79(l)	58
070	38.95	308(2)	238
140	40.35	185(2)	185
051	43.48	114(2)	105
160	47.82	82(l)	87
121	49.03	226(2)	210
090	50.76	134(l)	136
071	51.92	333(2)	657
141	53.04	397(l)	400

The temperature dependence of the intensity of the magnetic peak $(0\,1\,0)_M$, reported in Fig. 5, gives an ordering temperature $T_N = 7.2(2)$ K. This value is in agreement with that determined by magnetization measurements $T_N = 7.2(2)$ K.

The magnetic structure of $Ce_3Ni_2Ge_7$ is shown in Fig. 3b. In this ternary germanide, the layers of trigonal prisms [$Ce2_6$] are separated along the **b**-axis by two layers of antiprisms [$Ce2_4Ge_4$] and one layer of cubooctahedron [Ge_{12}] where Ce1 atoms are located. In this view, its magnetic structure can be described by a stacking of ferromagnetic [$Ce2_6$] trigonal prisms with a + − + − sequence along the **b**-axis. Comparable magnetic arrangement was previously reported for binary stannide Ce_2Sn_5 crystallizing in a superstructure of $CeSn_3$ well known as intermediate valence compound [16]. In Ce_2Sn_5, Ce atoms occupy also two inequivalent crystallographic sites: Ce1 are localized inside a cubooctahedron [Sn_{12}] and Ce2 forms trigonal prisms [$Ce2_6$]. Below $T_N = 2.9$ K, the inelastic neutron spectroscopy measurements on Ce_2Sn_5 reveal the coexistence in this stannide of non-magnetic (Ce1) and magnetic (Ce2) cerium atoms. Ce2 atoms form a layer of ferromagnetic [$Ce2_6$] trigonal prisms whereas Ce1 atoms exhibit an intermediate valence behaviour.

3.4. X-ray absorption spectroscopy at the Ce L_{III} edge

Neutron powder diffraction performed on $Ce_3Ni_2Ge_7$ suggests that Ce1 atoms could be in intermediate valence state. In order to probe the 4f electronic state of the two inequivalent Ce atoms in this ternary germanide, we have performed X-ray absorption spectroscopy at the Ce L_{III} edge. The result is discussed in relation to that obtained on homologue ternary stannide $Ce_3Ni_2Sn_7$.

Fig. 6 shows at room temperature, the Ce L_{III} absorption edge for $Ce_3Ni_2Ge_7$ and $Ce_3Ni_2Sn_7$.

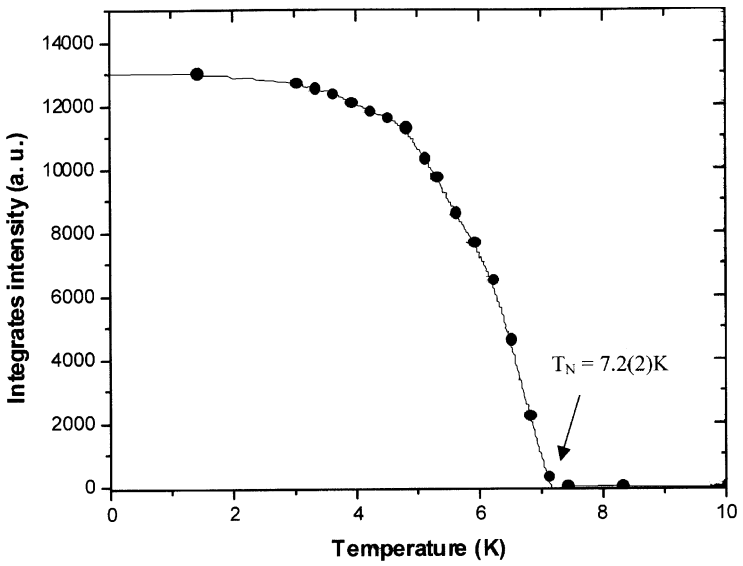

Fig. 5. Temperature dependence of the intensity of $(0\,1\,0)_M$ magnetic peak (dashed line is a guide for eye).

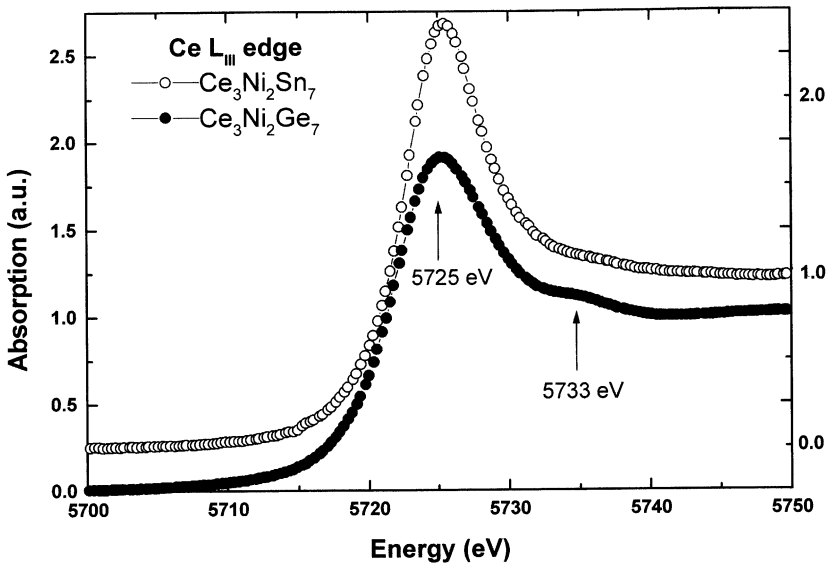

Fig. 6. Ce L_{III} absorption edge at room temperature for $Ce_3Ni_2Sn_7$ and $Ce_3Ni_2Ge_7$ (for clarity the spectrum relative to ternary stannide is shifted vertically).

For the stannide, a single strong peak located at 5725 eV is observed. The spectrum for the germanide clearly exhibits two resolved peaks separated by 8.5(6) eV. These peaks are due to optical transitions from a $2p_{3/2}$ electron to an empty 5d states in the presence of two different occupancies of the 4f shell ($4f^0$ and $4f^1$) in the final state [17]. The presence of two $4f^0$ and $4f^1$ configurations bears witness to the persistence of an intermediate valence state in $Ce_3Ni_2Ge_7$. Also, it is clear that the

white line of Ce L_{III} absorption edge in $Ce_3Ni_2Sn_7$ is very high and this demonstrates a very localized state of the 4f electronic shell.

An analysis of the Ce L_{III} absorption edge, described in detail in Ref. [18], has allowed to determine the average valence (v) of cerium in these two ternary compounds: $v = 3.00(1)$ for $Ce_3Ni_2Sn_7$ and $v = 3.03(1)$ for $Ce_3Ni_2Ge_7$. The latter value is very similar to that determined for $CeSn_3$ [17]. Keeping in mind that two inequivalent crystallographic sites are observed for Ce atoms in the germanide, two hypothesis are possible: (i) either the two Ce sites exhibit an intermediate valence state; (ii) or one exhibits a trivalent state whereas the other one is characterized by an intermediate valence state. The pronounced localized character of the 4f electronic states and the magnetic measurements carried out on $Ce_3Ni_2Ge_7$ play in favour of the second hypothesis.

4. Conclusion

The existence of two inequivalent crystallographic sites for Ce atoms in $Ce_3Ni_2Ge_7$ shows an interesting magnetic structure: Ce2 atom bears an ordered magnetic moment $1.98(2)\,\mu_B$ comparable to that expected for Ce^{3+} free ion ($g_J = 2.14\,\mu_B$) whereas Ce1 atom exhibits no magnetic moment. Crystallographic consideration (shorter Ce1–Ge distances), magnetization measurements and X-ray absorption spectroscopy experiment suggest an intermediate valence state for Ce1 species. In other words, $Ce_3Ni_2Ge_7$ (coexistence of magnetic and intermediate valence cerium atoms) can be considered as compound presenting a distribution of Kondo temperatures T_K as for instance Ce_2Sn_5, Ce_7Ni_3, etc. [19].

The character of a distinct valence for cerium in $Ce_3Ni_2Sn_7$ appears less obvious: X-ray absorption spectroscopy shows a trivalent state for the two Ce atoms. In this view, neutron powder diffraction experiments are in progress on this ternary stannide, to determine whether its magnetic structure at low temperature is either identical or different from that of $Ce_3Ni_2Ge_7$.

References

[1] P. Salamakha, M. Konyk, O. Sologub, O. Bodak, J. Alloys Compounds 236 (1996) 206.
[2] R.V. Skolozdra, in: K. A. Gschneidner Jr., L. Eyring, (Eds.), Handbook on the Physics and Chemistry of Rare Earths, Vol. 24, Elsevier, North-Holland, 1997, p. 399.
[3] B. Chevalier, J. Etourneau, J. Mater. Chem. 9 (1999) 1789.
[4] J.P. Kuang, H.J. Cui, J.Y. Li, F.M. Yang, H. Nakotte, E. Brück, F.R. de Boer, J. Magn. Magn. Mater. 104–107 (1992) 1475.
[5] T. Takabatake, F. Teshima, H. Fujii, S. Nishigori, T. Suzuki, T. Fujita, Y. Yamaguchi, J. Sakurai, D. Jaccard, Phys. Rev. B 41 (1990) 9607.
[6] P. Gegenwart, F. Kromer, M. Lang, G. Sparn, C. Geibel, F. Steglich, Phys. Rev. Lett. 82 (1999) 1293.
[7] T. Takabatake, F. Teshima, H. Fujii, S. Nishigori, T. Suzuki, T. Fujita, Y. Yamaguchi, J. Sakurai, J. Magn. Magn. Mater. 90–91 (1990) 474.
[8] W.P. Beyermann, M.F. Hundley, P.C. Canfield, J.D. Thompson, M. Latroche, C. Godart, M. Selsane, Z. Fisk, J.L. Smith, Phys. Rev. B 43 (1991) 13130.
[9] J. Rodriguez-Carvajal, Powder Diffraction, Satellite Meeting of the 15th Congress of IUCr, Toulouse, France, 1990, p. 127.
[10] V.F. Sears, Neutron News 3 (3) (1992) 26.
[11] A.J. Freeeman, J.P. Desclaux, J. Magn. Magn. Mater. 12 (1979) 11.
[12] V.K. Pecharsky, K.A. Gschneidner Jr., L.L. Miller, Phys. Rev. B 43 (1991) 10906.
[13] P. Schobinger-Papamantellos, A. Krimmel, A. Grauel, K.H.J. Buschow, J. Magn. Magn. Mater. 125 (1993) 151.
[14] B. Chevalier, J. Etourneau, J. Magn. Magn. Mater. 196–197 (1999) 880.
[15] E.F. Bertaut, Acta Crystallogr. A 24 (1968) 217.
[16] M. Bonnet, J.X. Boucherle, F. Givord, F. Lapierre, P. Lejay, J. Odin, A.P. Murani, J. Schweizer, A. Stunault, J. Magn. Magn. Mater. 132 (1994) 289.
[17] D. Wohlleben, J. Röhler, J. Appl. Phys. 55 (1984) 1904.
[18] O. Isnard, S. Miraglia, J. Buschow, J. Synchrotron Radiat. 6 (1999) 703.
[19] K.A. Gschneidner Jr., V.K. Pecharsky, Physica B 223–224 (1996) 131.